EUROPEAN ORGANISATION FOR NUCLEAR RESEARCH

CERN-PPE/96-90
27 June 1996

Multiplicity Dependence of Bose–Einstein Correlations in Hadronic Z^0 Decays

The OPAL Collaboration

Abstract

Bose–Einstein correlations between like charged track pairs have been studied using a sample of approximately 3.6 million multihadronic Z^0 decays collected with the OPAL detector at LEP. The radius of the emitting source R and the chaoticity parameter λ were studied using two parametrisations, the Goldhaber (G) parametrisation and the one-dimensional Kopylov-Podgoretskiĭ (KP) parametrisation. The radii R_{G} and R_{KP} are found to increase linearly with the average observed charged multiplicity n_{ch}, with changes with respect to a unit increase in n_{ch} of

$$\frac{1}{\langle R_{\mathrm{G}}\rangle}\frac{\Delta R_{\mathrm{G}}}{\Delta n_{ch}} = (3.6 \pm 0.6)\cdot 10^{-3} \quad \text{and} \quad \frac{1}{\langle R_{\mathrm{KP}}\rangle}\frac{\Delta R_{\mathrm{KP}}}{\Delta n_{ch}} = (3.4 \pm 1.0)\cdot 10^{-3},$$

where the $\langle R\rangle$ are the radius values measured in the inclusive event sample. The chaoticity parameters λ_{G} and λ_{KP} decrease with increasing charged multiplicity. It is shown that the increase of R with multiplicity may be connected with differences between two- and three-jet events.

(Submitted to Z. Phys.)

The OPAL Collaboration

G. Alexander[23], J. Allison[16], N. Altekamp[5], K. Ametewee[25], K.J. Anderson[9], S. Anderson[12], S. Arcelli[2], S. Asai[24], D. Axen[29], G. Azuelos[18,a], A.H. Ball[17], E. Barberio[8], R.J. Barlow[16], R. Bartoldus[3], J.R. Batley[5], J. Bechtluft[14], C. Beeston[16], T. Behnke[8], A.N. Bell[1], K.W. Bell[20], G. Bella[23], S. Bentvelsen[8], P. Berlich[10], S. Bethke[14], O. Biebel[14], V. Blobel[8], I.J. Bloodworth[1], J.E. Bloomer[1], M. Bobinski[10], P. Bock[11], H.M. Bosch[11], M. Boutemeur[34], B.T. Bouwens[12], S. Braibant[12], R.M. Brown[20], H.J. Burckhart[8], C. Burgard[8], R. Bürgin[10], P. Capiluppi[2], R.K. Carnegie[6], A.A. Carter[13], J.R. Carter[5], C.Y. Chang[17], C. Charlesworth[6], D.G. Charlton[1,b], D. Chrisman[4], S.L. Chu[4], P.E.L. Clarke[15], I. Cohen[23], J.E. Conboy[15], O.C. Cooke[16], M. Cuffiani[2], S. Dado[22], C. Dallapiccola[17], G.M. Dallavalle[2], S. De Jong[12], L.A. del Pozo[8], K. Desch[3], M.S. Dixit[7], E. do Couto e Silva[12], M. Doucet[18], E. Duchovni[26], G. Duckeck[34], I.P. Duerdoth[16], J.E.G. Edwards[16], P.G. Estabrooks[6], H.G. Evans[9], M. Evans[13], F. Fabbri[2], P. Fath[11], F. Fiedler[12], M. Fierro[2], H.M. Fischer[3], R. Folman[26], D.G. Fong[17], M. Foucher[17], A. Fürtjes[8], P. Gagnon[7], A. Gaidot[21], J.W. Gary[4], J. Gascon[18], S.M. Gascon-Shotkin[17], N.I. Geddes[20], C. Geich-Gimbel[3], F.X. Gentit[21], T. Geralis[20], G. Giacomelli[2], P. Giacomelli[4], R. Giacomelli[2], V. Gibson[5], W.R. Gibson[13], D.M. Gingrich[30,a], D. Glenzinski[9], J. Goldberg[22], M.J. Goodrick[5], W. Gorn[4], C. Grandi[2], E. Gross[26], M. Gruwé[8], C. Hajdu[32], G.G. Hanson[12], M. Hansroul[8], M. Hapke[13], C.K. Hargrove[7], P.A. Hart[9], C. Hartmann[3], M. Hauschild[8], C.M. Hawkes[5], R. Hawkings[8], R.J. Hemingway[6], G. Herten[10], R.D. Heuer[8], M.D. Hildreth[8], J.C. Hill[5], S.J. Hillier[1], T. Hilse[10], P.R. Hobson[25], R.J. Homer[1], A.K. Honma[28,a], D. Horváth[32,c], R. Howard[29], R.E. Hughes-Jones[16], D.E. Hutchcroft[5], P. Igo-Kemenes[11], D.C. Imrie[25], M.R. Ingram[16], K. Ishii[24], A. Jawahery[17], P.W. Jeffreys[20], H. Jeremie[18], M. Jimack[1], A. Joly[18], C.R. Jones[5], G. Jones[16], M. Jones[6], R.W.L. Jones[8], U. Jost[11], P. Jovanovic[1], T.R. Junk[8], D. Karlen[6], K. Kawagoe[24], T. Kawamoto[24], R.K. Keeler[28], R.G. Kellogg[17], B.W. Kennedy[20], B.J. King[8], J. Kirk[29], S. Kluth[8], T. Kobayashi[24], M. Kobel[10], D.S. Koetke[6], T.P. Kokott[3], S. Komamiya[24], R. Kowalewski[8], T. Kress[11], P. Krieger[6], J. von Krogh[11], P. Kyberd[13], G.D. Lafferty[16], H. Lafoux[21], R. Lahmann[17], W.P. Lai[19], D. Lanske[14], J. Lauber[15], S.R. Lautenschlager[31], J.G. Layter[4], D. Lazic[22], A.M. Lee[31], E. Lefebvre[18], D. Lellouch[26], J. Letts[2], L. Levinson[26], C. Lewis[15], S.L. Lloyd[13], F.K. Loebinger[16], G.D. Long[17], M.J. Losty[7], J. Ludwig[10], A. Luig[10], A. Malik[21], M. Mannelli[8], S. Marcellini[2], C. Markus[3], A.J. Martin[13], J.P. Martin[18], G. Martinez[17], T. Mashimo[24], W. Matthews[25], P. Mättig[3], W.J. McDonald[30], J. McKenna[29], E.A. Mckigney[15], T.J. McMahon[1], A.I. McNab[13], R.A. McPherson[8], F. Meijers[8], S. Menke[3], F.S. Merritt[9], H. Mes[7], J. Meyer[27], A. Michelini[2], G. Mikenberg[26], D.J. Miller[15], R. Mir[26], W. Mohr[10], A. Montanari[2], T. Mori[24], M. Morii[24], U. Müller[3], K. Nagai[26], I. Nakamura[24], H.A. Neal[8], B. Nellen[3], B. Nijjhar[16], R. Nisius[8], S.W. O'Neale[1], F.G. Oakham[7], F. Odorici[2], H.O. Ogren[12], T. Omori[24], M.J. Oreglia[9], S. Orito[24], J. Pálinkás[33,d], G. Pásztor[32], J.R. Pater[16], G.N. Patrick[20], J. Patt[10], M.J. Pearce[1], S. Petzold[27], P. Pfeifenschneider[14], J.E. Pilcher[9], J. Pinfold[30], D.E. Plane[8], P. Poffenberger[28], B. Poli[2], A. Posthaus[3], H. Przysiezniak[30], D.L. Rees[1], D. Rigby[1], S.A. Robins[13], N. Rodning[30], J.M. Roney[28], A. Rooke[15], E. Ros[8], A.M. Rossi[2], M. Rosvick[28], P. Routenburg[30], Y. Rozen[22], K. Runge[10], O. Runolfsson[8], U. Ruppel[14], D.R. Rust[12], R. Rylko[25], K. Sachs[10], E.K.G. Sarkisyan[23], M. Sasaki[24], C. Sbarra[2], A.D. Schaile[34], O. Schaile[34], F. Scharf[3], P. Scharff-Hansen[8], P. Schenk[4], B. Schmitt[8], S. Schmitt[11], M. Schröder[8], H.C. Schultz-Coulon[10], M. Schulz[8], M. Schumacher[3], P. Schütz[3], W.G. Scott[20], T.G. Shears[16], B.C. Shen[4], C.H. Shepherd-Themistocleous[27], P. Sherwood[15], G.P. Siroli[2], A. Sittler[27], A. Skillman[15], A. Skuja[17], A.M. Smith[8], T.J. Smith[28],

G.A. Snow[17], R. Sobie[28], S. Söldner-Rembold[10], R.W. Springer[30], M. Sproston[20], A. Stahl[3], M. Starks[12], M. Steiert[11], K. Stephens[16], J. Steuerer[27], B. Stockhausen[3], D. Strom[19], F. Strumia[8], P. Szymanski[20], R. Tafirout[18], S.D. Talbot[1], S. Tanaka[24], P. Taras[18], S. Tarem[22], M. Tecchio[8], M. Thiergen[10], M.A. Thomson[8], E. von Törne[3], S. Towers[6], T. Tsukamoto[24], E. Tsur[23], A.S. Turcot[9], M.F. Turner-Watson[8], P. Utzat[11], R. Van Kooten[12], G. Vasseur[21], M. Verzocchi[10], P. Vikas[18], M. Vincter[28], E.H. Vokurka[16], F. Wäckerle[10], A. Wagner[27], C.P. Ward[5], D.R. Ward[5], J.J. Ward[15], P.M. Watkins[1], A.T. Watson[1], N.K. Watson[7], P. Weber[6], P.S. Wells[8], N. Wermes[3], J.S. White[28], B. Wilkens[10], G.W. Wilson[27], J.A. Wilson[1], G. Wolf[26], S. Wotton[5], T.R. Wyatt[16], S. Yamashita[24], G. Yekutieli[26], V. Zacek[18],

[1]School of Physics and Space Research, University of Birmingham, Birmingham B15 2TT, UK
[2]Dipartimento di Fisica dell' Università di Bologna and INFN, I-40126 Bologna, Italy
[3]Physikalisches Institut, Universität Bonn, D-53115 Bonn, Germany
[4]Department of Physics, University of California, Riverside CA 92521, USA
[5]Cavendish Laboratory, Cambridge CB3 0HE, UK
[6] Ottawa-Carleton Institute for Physics, Department of Physics, Carleton University, Ottawa, Ontario K1S 5B6, Canada
[7]Centre for Research in Particle Physics, Carleton University, Ottawa, Ontario K1S 5B6, Canada
[8]CERN, European Organisation for Particle Physics, CH-1211 Geneva 23, Switzerland
[9]Enrico Fermi Institute and Department of Physics, University of Chicago, Chicago IL 60637, USA
[10]Fakultät für Physik, Albert Ludwigs Universität, D-79104 Freiburg, Germany
[11]Physikalisches Institut, Universität Heidelberg, D-69120 Heidelberg, Germany
[12]Indiana University, Department of Physics, Swain Hall West 117, Bloomington IN 47405, USA
[13]Queen Mary and Westfield College, University of London, London E1 4NS, UK
[14]Technische Hochschule Aachen, III Physikalisches Institut, Sommerfeldstrasse 26-28, D-52056 Aachen, Germany
[15]University College London, London WC1E 6BT, UK
[16]Department of Physics, Schuster Laboratory, The University, Manchester M13 9PL, UK
[17]Department of Physics, University of Maryland, College Park, MD 20742, USA
[18]Laboratoire de Physique Nucléaire, Université de Montréal, Montréal, Quebec H3C 3J7, Canada
[19]University of Oregon, Department of Physics, Eugene OR 97403, USA
[20]Rutherford Appleton Laboratory, Chilton, Didcot, Oxfordshire OX11 0QX, UK
[21]CEA, DAPNIA/SPP, CE-Saclay, F-91191 Gif-sur-Yvette, France
[22]Department of Physics, Technion-Israel Institute of Technology, Haifa 32000, Israel
[23]Department of Physics and Astronomy, Tel Aviv University, Tel Aviv 69978, Israel
[24]International Centre for Elementary Particle Physics and Department of Physics, University of Tokyo, Tokyo 113, and Kobe University, Kobe 657, Japan
[25]Brunel University, Uxbridge, Middlesex UB8 3PH, UK
[26]Particle Physics Department, Weizmann Institute of Science, Rehovot 76100, Israel
[27]Universität Hamburg/DESY, II Institut für Experimental Physik, Notkestrasse 85, D-22607 Hamburg, Germany
[28]University of Victoria, Department of Physics, P O Box 3055, Victoria BC V8W 3P6, Canada

[29]University of British Columbia, Department of Physics, Vancouver BC V6T 1Z1, Canada
[30]University of Alberta, Department of Physics, Edmonton AB T6G 2J1, Canada
[31]Duke University, Dept of Physics, Durham, NC 27708-0305, USA
[32]Research Institute for Particle and Nuclear Physics, H-1525 Budapest, P O Box 49, Hungary
[33]Institute of Nuclear Research, H-4001 Debrecen, P O Box 51, Hungary
[34]Ludwigs-Maximilians-Universität München, Sektion Physik, Am Coulombwall 1, D-85748 Garching, Germany

[a] and at TRIUMF, Vancouver, Canada V6T 2A3
[b] and Royal Society University Research Fellow
[c] and Institute of Nuclear Research, Debrecen, Hungary
[d] and Department of Experimental Physics, Lajos Kossuth University, Debrecen, Hungary

1 Introduction

Correlations in phase space between identical bosons have been investigated over a wide range of centre-of-mass energies and different initial state reactions [1] and have been interpreted to be a consequence of Bose–Einstein (BE) statistics obeyed by identical pions, according to which identical bosons tend to be produced close to each other in phase space. The result is an enhancement in the number of like charged pairs, relative to the number of unlike charged pairs, of particles with similar momenta. The BE effect is generally parametrised in terms of a radius R of the pion emitting source and a chaoticity parameter λ which represents the strength of the effect. In a previous OPAL paper [2], based on a sample of 146,624 multihadronic Z^0 decays, a small increase in the radius of the emitting source with the charged multiplicity of the event was observed. Due to the low statistics available at the time the multiplicity distribution was divided into only two ranges. In other e^+e^- experiments, searches for such a dependence have not found any effect [3, 4]; the statistics available in those analyses were rather low, and were probably not sufficient to find the small effect presented in this paper. However, in hadron-hadron collisions, an increase in the radius with increasing multiplicity has been measured in experiments with centre-of-mass energies $\sqrt{s} \geq 30$ GeV [5, 6, 7]. This effect has also been observed in heavy ion collisions [8]. It is therefore interesting to use the high statistics data available at LEP to establish whether a similar effect can be seen in the much simpler hadronization environment of e^+e^- annihilations.

BE correlations can be described in terms of a correlation function

$$C(p_1, p_2) = \frac{\rho(p_1, p_2)}{\rho_0(p_1, p_2)}, \tag{1}$$

where p_1 and p_2 are the four-momenta of the two pions, $\rho(p_1, p_2) = (1/\sigma)(d^8\sigma/d^4p_1 d^4p_2)$ is the measured density of the two pions, and $\rho_0(p_1, p_2)$ is the two-particle density in the absence of BE correlations. The choice of a reference sample to determine $\rho_0(p_1, p_2)$ is therefore crucial for the measurement. Ideally it should have the same properties as the sample $\rho(p_1, p_2)$ except for the presence of BE correlations. It should contain any other relevant correlations, such as those due to energy-momentum and charge conservation, the topology, global event properties and resonances of the sample $\rho(p_1, p_2)$.

In this analysis, the first sample consists of like charged pairs. The second sample, called the reference sample, is composed of unlike charged pairs. The reference sample formed by pairing particles from the same event has the requirements mentioned before but is affected by the presence of dynamical correlations due to the decay products of weakly-decaying and resonant particles, such as K^0_S, ρ^0, ω, and η, which do not affect the sample $\rho(p_1, p_2)$. The presence of these decay products in the reference sample introduces systematic effects in the correlation function, as discussed in Section 3. We have not considered the effects of BE correlation on the $\pi^+\pi^-$ reference sample, which arise as an indirect reflection of the BE correlations in the like charged pairs sample into the unlike charged pairs sample, due to the topological jet structure of the events [9]. Checks were made using a Monte Carlo simulation to construct the reference sample. We noticed that it was not possible to exclude the effects of the resonance decay products: these checks are described in Section 3.1. We have not used a mixed event technique, because such technique could not preserve the dynamical correlations between particles, such as the energy–momentum conservation.

Following our previous paper [2], we measure the "distance" in phase space using the modulus of the four-momentum difference of the pair, $Q^2 = -q^2 = -(p_1 - p_2)^2$. Various

parametrisations of the correlation function, $C(Q)$, which assume different shapes for the pion emitting source, can be found in the literature. In this study we use the following two:

- The Goldhaber (G) or gaussian parametrisation [10], which assumes a spherical shape with a radial gaussian distribution of the emitting source,

$$C(Q) = N_{\rm G}\,(1 + \lambda_{\rm G} {\rm e}^{-Q^2 R_{\rm G}^2})\,(1 + \delta_{\rm G}\,Q + \epsilon_{\rm G}\,Q^2), \tag{2}$$

  where $R_{\rm G}$ is a measure of the radius of this source. The parameter $\lambda_{\rm G}$ represents the strength of the correlation, with $0 \leq \lambda_{\rm G} \leq 1$. A value of $\lambda_{\rm G} = 1$ corresponds to a fully chaotic source, while $\lambda_{\rm G} = 0$ corresponds to a completely coherent source. The empirical term $(1 + \delta_{\rm G}\,Q + \epsilon_{\rm G}\,Q^2)$ takes into account the behaviour of the correlation function at high Q values due to long range particle correlations. $N_{\rm G}$ is a normalization factor. This parametrisation has the advantage of being Lorentz invariant.

- The Kopylov–Podgoretskiĭ (KP) parametrisation [11, 12], which assumes that the source of interfering pions is a spherical surface populated with a uniform density of point-like pion radiators of lifetime τ,

$$C(q_t, q_0) = 1 + \lambda_{\rm KP}\,[2\,J_1(R_{\rm KP}\,q_t)/(R_{\rm KP}\,q_t)]^2/(1 + q_0^2\tau^2), \tag{3}$$

  where J_1 is the first order Bessel function, q_t is the modulus of the transverse component of $\vec{q} = \vec{p_1} - \vec{p_2}$ with respect to $\vec{p_1} + \vec{p_2}$ ($\vec{p_i}$ being the particle three-momentum vector), $q_0 = |E_1 - E_2|$, E_i being the energy of one particle of the pair, $R_{\rm KP}$ is the emitting source radius, and $\lambda_{\rm KP}$ is the BE correlation strength. The parameter τ multiplied by the speed of light c could be interpreted as the effective thickness of the emitting source. To increase the statistics for the measurements of the dependence of $R_{\rm KP}$ and $\lambda_{\rm KP}$ on the charged multiplicity of the event, we use a one-dimensional parametrisation derived from Eq. 3 (See Ref. [5, 13]), by restricting the allowed energy difference to $q_0 \leq q_{0\,max}$, which gives:

$$C(q_t) = N_{\rm KP}\,\left[1 + \lambda_{\rm KP}\,[2\,J_1(R_{\rm KP}\,q_t)/(R_{\rm KP}\,q_t)]^2\right]\,(1 + \delta_{\rm KP}\,q_t + \epsilon_{\rm KP}\,q_t^2). \tag{4}$$

  The cut on q_0 should enhance the BE effect since the correlations are expected to become stronger as $q_0 \to 0$. An empirical long range correlation factor and a normalization factor $N_{\rm KP}$ are also needed, as in the G parametrisation.

Since the G and KP parametrisations assume two different radial dependences for the source, the values of the two radii $R_{\rm KP}$ and $R_{\rm G}$ are expected to be different. In particular $R_{\rm KP}$ is usually larger than the radius $R_{\rm G}$ [3, 13]. The correlation strength parameter $\lambda_{\rm G}$ is expected to be approximately equal to $\lambda_{\rm KP}$.

The OPAL detector, the event selection, and the charged track selection criteria are described in Section 2. In Section 3 the measurements of the radii $R_{\rm G}$ and $R_{\rm KP}$ and the chaoticity parameters $\lambda_{\rm KP}$ and $\lambda_{\rm G}$ for the entire event sample are described. The dependence of the radii and chaoticity parameters on the observed charged multiplicity are then investigated in Section 4, and conclusions are presented in Section 5.

2 Detector and data selection

The OPAL detector has been described in detail in Ref. [14, 15]. The present analysis is based mainly on the information from the central tracking chambers, which consist of a silicon

microvertex detector, a vertex chamber, a jet chamber with 159 layers of axial anode wires, and outer chambers to improve the z coordinate resolution. These detectors are located in a 0.435 T axial magnetic field and measure p_t, the transverse track momentum with respect to the beam axis, with a precision of $(\sigma_{p_t}/p_t) = \sqrt{(0.02)^2 + (0.0015\,p_t)^2}$ (p_t in GeV/c) for $|\cos\theta| < 0.73$, where θ is the polar angle of the track[1]. The jet chamber also measures the specific energy loss of charged particles, $\mathrm{d}E/\mathrm{d}x$, with a resolution $\sigma(\mathrm{dE/dx})/(\mathrm{dE/dx}) \simeq 3.5\%$ (for a track having 159 hits in the jet chamber). The energy loss $\mathrm{d}E/\mathrm{d}x$ is used to identify charged particles [16]. The OPAL trigger system is described in Ref. [17] and the selection procedures for multihadronic events are discussed in Ref. [18]. A sample of 2.6 million simulated Monte Carlo events, generated with JETSET 7.3 and with parameters to fit OPAL data [19, 20], and including a full simulation of the detector [21], was used to measure the efficiencies of track and event rejection as detailed below.

Charged tracks were required to satisfy a number of criteria which may be divided into two classes. The first set of selections defines the general track quality and the second set is specific to this analysis. The first set requires that charged tracks have at least 20 hits in the jet chamber, a minimum transverse momentum p_t of 0.15 GeV/c, a maximum measured momentum p of 65 GeV/c, and a measured distance of closest approach to the origin of less than 5 cm in the $r-\phi$ plane, and less than 200 cm in the z direction. The polar angle of the thrust axis, calculated using charged tracks that passed the above cuts, had to satisfy $|\cos\theta_{\mathrm{thrust}}| < 0.9$ in order to accept only events which were well-contained in the detector. After these selections, the number of charged tracks in each event, n_{ch}, was calculated. The average observed charged multiplicity n_{ch} is about a factor 1.023 smaller than the corrected charged multiplicity [22].

The second set of cuts was applied to events and tracks which passed the first set. A track was required to have $p < 40$ GeV/c and at least 20 hits in the jet chamber which were useful for the $\mathrm{d}E/\mathrm{d}x$ measurement. We used a $\mathrm{d}E/\mathrm{d}x$ track selection only for a systematic check of the dependence of the results on the pion sample purity, as explained in Section 3.1. In addition, each track was required to originate from the primary vertex of the interaction calculated on an event by event basis using all charged tracks [23]. About 67% of photon conversion pairs were rejected [24], reducing the conversion background in the sample to less than 0.1% of the number of tracks. The fraction of pions in the track sample was about 79% as evaluated from a Monte Carlo simulation.

After these cuts, all events with fewer than five charged tracks were rejected and the difference between the number of positively and negatively charged tracks was required to be less than 40% of the total number of charged tracks, in order to avoid unbalanced numbers of like charged and unlike charged pairs. Starting from a sample of 3,606,647 multihadronic events, a total of 3,090,142 events passed the selection criteria.

3 Analysis

Using the tracks that passed the cuts mentioned above, pairs were formed to determine the correlation function $C(Q)$. Coulomb interactions between charged particles affect like and unlike charged pairs in opposite ways and modify the correlation function. We therefore applied the

[1] The OPAL coordinate system is defined so that z is the coordinate parallel to the beam axis in the direction of the incoming electron beam, r is the coordinate normal to the beam axis, ϕ is the azimuthal angle and θ is the polar angle with respect to z.

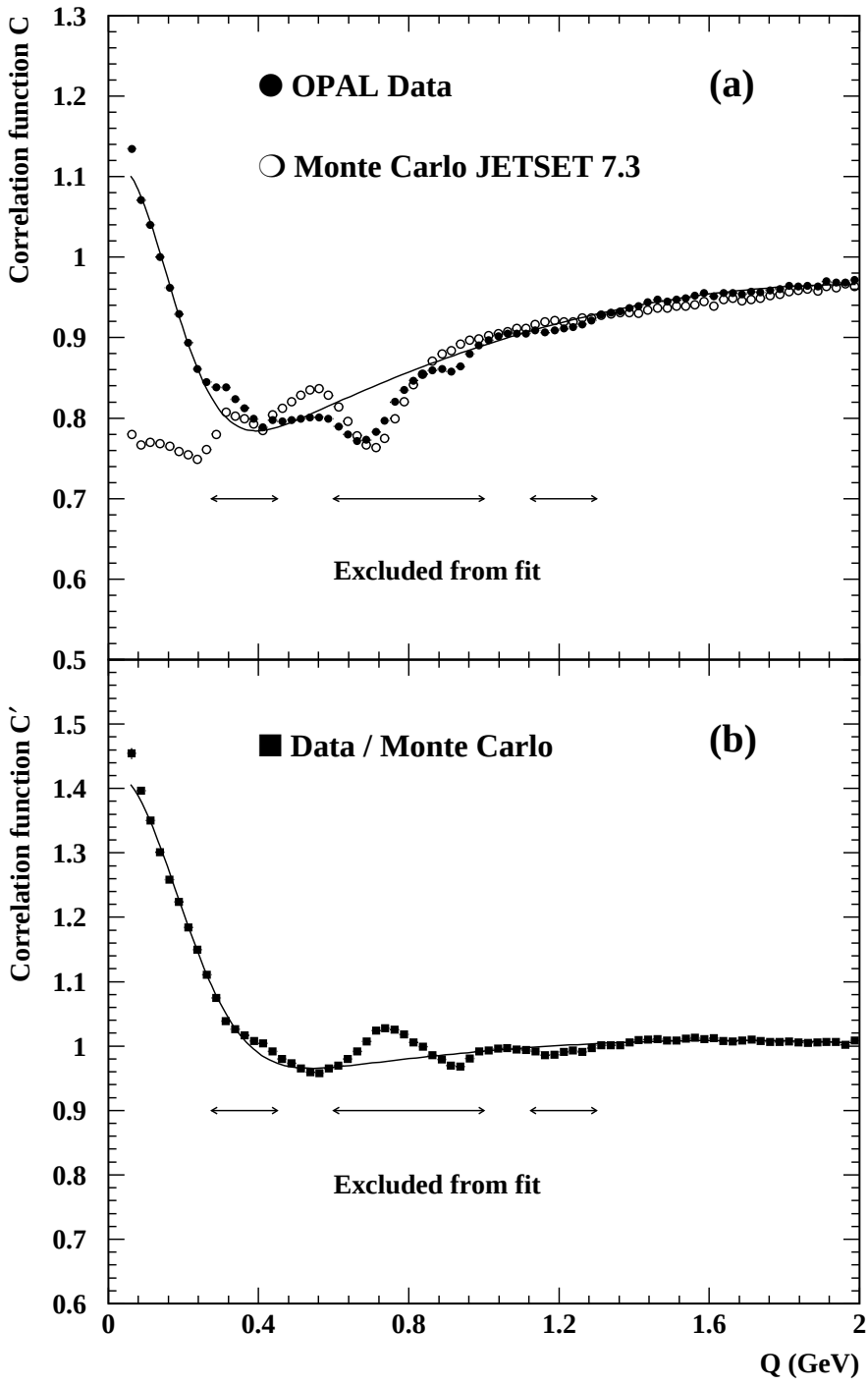

Figure 1: (a) The correlation function $C(Q)$ for like charged pairs relative to unlike charged pairs. The Coulomb–corrected data are shown as solid points and the Monte Carlo events with full detector simulation as open points. (b) The correlation function $C'(Q)$ obtained by dividing the two distributions in (a). In (a) and (b) the solid lines show the fits of the G parametrisation to the data. The regions excluded from the reference fits are indicated in the figures. The error bars represent the statistical uncertainties.

following correction as a function of Q [25] to the correlation function,

$$C_{corr}(Q) = \chi(Q) C_{uncorr}(Q) \ , \tag{5}$$

where $\chi(Q)$ is

$$\chi(Q) = \frac{e^{2\pi\eta} - 1}{1 - e^{-2\pi\eta}} \ , \tag{6}$$

and where $\eta = \alpha m_\pi / Q$, α is the fine-structure constant and m_π is the charged pion mass. The correction factor $\chi(Q)$ is about 11% in the first fitted bin, 8% in the second bin and about 3% in the tenth bin. Alternative Coulomb corrections [26, 27] have been proposed, which lead to different parametrisations of the correlation function; however, to remain consistent with the other published experimental data, these were not applied in this analysis. The Monte Carlo program does not contain a simulation of Coulomb effects, so the Monte Carlo distributions were not corrected by Eq. 5.

The resulting $C(Q)$ is shown in Fig. 1a, for data and for Monte Carlo simulated events which do not contain BE correlations. The experimental data exhibit a clear enhancement at low Q, as expected from BE correlations, while in the Monte Carlo data set no such effect is observed.

3.1 Results using the Goldhaber parametrisation

A minimum χ^2 fit of Eq. 2 to the data was performed over the range $0.05 \leq Q \leq 2.0$ GeV excluding the resonance regions, as illustrated in Fig. 1a. The region $Q < 0.05$ GeV was excluded to avoid problems of detector resolution and badly reconstructed or split tracks which mimic two like charged tracks with a very low Q value. It was verified using the Monte Carlo simulation that the majority of such tracks affects the region $Q < 0.05$ GeV of like charged distributions.

The regions $0.275 < Q < 0.45$ GeV, $0.6 < Q < 1.0$ GeV, and $1.1 < Q < 1.3$ GeV were excluded from the fits because of large distortions in the correlation function, as can be seen in Fig. 1a. These distortions are caused primarily by the decay products of K^0_S, ω, η, and η' in the first range, ρ^0 and $f_0(975)$ in the second, and $f_2(1270)$ in the third. From Monte Carlo simulations, after excluding the above regions from the fit, it was estimated that the number of accepted pairs in which both tracks are decay products of particles containing b or c quarks was less than 1%. The result of the fit[2] of the G parametrisation is given in line (a) of Table 1.

Many final state pions in multihadronic events result from decays of short-lived particles, such as K^0_S, although the requirement that a particle should come from the primary interaction vertex reduced the number of pions from such secondary sources. Since these pions do not exhibit any BE effects, the correlation strength λ_G is reduced.

The large values of χ^2 arise from distortions in the data caused by the presence of resonance decay products. As can be seen in Fig. 1a, some structure in the correlation function which was not visible with the lower statistics of Ref. [2] can now be seen outside the regions which were excluded from the fit. A study found that they account for most of the χ^2, because the parametrisation cannot accommodate these structures. In contrast to this the parametrisation function fits the data well in the BE enhancement region ($Q < 0.275$ GeV). In order to obtain a meaningful statistical uncertainty from the fits, we have scaled the fit errors by $\sqrt{\chi^2/\text{d.o.f.}}$ [28].

[2] The other parameter values of the fit are $\delta_G = 0.4349 \pm 0.0042\,\text{GeV}^{-1}$, $\epsilon_G = -0.1054 \pm 0.0017\,\text{GeV}^{-2}$ and $N_G = 0.6681 \pm 0.0012$, where the errors are those from the fit, not scaled by $(\chi^2/\text{d.o.f.})^{1/2}$.

	$R_{\rm G}$ (fm)	$\lambda_{\rm G}$	χ^2/d.o.f.
a) Reference fit	0.955 ± 0.012	0.672 ± 0.013	402/40
b) Different resonance regions excl.	0.944 ± 0.011	0.653 ± 0.013	600/49
c) Modified track selection	0.948 ± 0.011	0.677 ± 0.013	398/40
d) Q binning = 50 MeV	0.962 ± 0.013	0.667 ± 0.014	204/17
e) $0.05 \leq Q \leq 1.5$ GeV	0.952 ± 0.015	0.685 ± 0.024	342/20
f) Reference sample from Monte Carlo	0.793 ± 0.015	0.577 ± 0.010	185/40

Table 1: Results of several fits of the G parametrisation to the data, with statistical errors. These results were used to estimate the overall systematic uncertainties on the parameters. The differences between the parameter values of the reference fit (a) and the others from (b) to (e) were added in quadrature to obtain an estimate of the systematic uncertainties on $R_{\rm G}$ and $\lambda_{\rm G}$. The significance of the large values of χ^2/d.o.f. is discussed in the text, and the errors have been scaled by $(\chi^2/\text{d.o.f.})^{1/2}$.

As a check we divided the data into 5 equal-sized subsamples and found that the variance of the values of R and λ agreed with this determination of the statistical error.

In order to estimate the systematic effects arising from the resonance decay products, another fit was made excluding the resonance regions $0.3 < Q < 0.45$ GeV, $0.6 < Q < 1.0$ GeV, corresponding roughly to the fit already used in [2] (fit (b) in Table 1). This included in the fit the region distorted by the $f_2(1270)$: with the low statistics available in [2], no distortions were visible in this high Q region and thus it was not excluded. The result of the fit indicates that the shifts in the fitted parameter values are small.

The analysis was repeated changing the track selection criteria described in Section 2, in order to estimate systematic effects related to track and event selection (fit (c) in Table 1). In particular we required a track to have $p < 30$ GeV/c, at least 30 hits in the tracking chambers useful for the $\mathrm{d}E/\mathrm{d}x$ measurement, and we required an event to have the difference between the number of positively and negatively charged tracks to be less than 25% of the total number of charged tracks. Again, the shifts in the fitted values are observed to be small.

Another source of systematic error is the energy-momentum resolution, since a poor resolution can smear the correlation function $C(Q)$. From Monte Carlo simulations it has been estimated that the resolution of the Q variable is about 25 MeV, independent of the track direction and of the relative charge sign. Even if this resolution is marginally worse for the data, this effect is negligible because the Q-region that exhibits the BE correlation enhancement has a range of the order of hundreds of MeV. The bin size was therefore chosen to be 25 MeV. A study of possible systematic effects due to the choice of the binning was performed by changing the bin size from 25 MeV to 50 MeV (fit (d) of Table 1).

The high Q-value region of the fit is affected by long-range correlations. These correlations should induce the same effects in the like charged pairs and in the reference sample. In order to estimate how these correlations could modify our results, a fit was performed in a more restricted interval, from $0.05 \leq Q \leq 1.5$ GeV (fit (e) in Table 1). The values of the fitted parameters show small changes from those of the reference fit.

In order to estimate the effect of the choice of the reference sample, we used the Monte Carlo event sample, which does not include a simulation of the BE effect, to construct a ratio

of correlation functions:

$$C'(Q) = \frac{C^{data}(Q)}{C^{MC}(Q)} \tag{7}$$

The simulation includes many of the dynamical correlations present in the real data. In particular it includes many resonance decay products, which, if properly modelled, would result in removing from $C'(Q)$ the structure due to the resonances. The Q dependence of $C'(Q)$ is shown in Fig. 1b. The result of the fit of the G parametrisation to this new correlation function Eq. 7 is given in line (f) of Table 1. The χ^2 of the fit improves significantly, both because of the larger errors on each point (which is now a ratio between two numbers with approximately the same statistical error) and because many of the resonance structures are removed. Note, however, that not all the resonances are modelled correctly or included in the Monte Carlo simulation. In particular the shape of the ρ^0 is badly modelled, which is probably an effect of the omission of BE correlations in the simulations [9, 29]. Also, the JETSET version used does not include all of the meson resonances, such as the $f_2(1270)$. Since the Monte Carlo sample does not remove resonance problems, those regions are omitted from the fit anyway. Since the use of the Monte Carlo sample does not remove the problems related to the decay products, we did not use the results of the fit of Eq. 7 to estimate the systematic error, in contrast to our previous paper [2]. In any case, since the main thrust of the present analysis is to study the R and λ dependence on observed charged multiplicity, we concentrate on the fits obtained with the reference sample from data.

The results of these fits were used to estimate the systematic errors on each of the parameters by summing in quadrature the differences in the parameter values between these fits (b)–(e) and the reference fit (a). The final results of the parameters $R_{\rm G}$ and $\lambda_{\rm G}$ in the G parametrisation are:

$$R_{\rm G} = 0.955 \pm 0.012 \pm 0.015\,{\rm fm}, \qquad \lambda_{\rm G} = 0.672 \pm 0.013 \pm 0.024,$$

where the first errors are statistical and the second are estimates of systematic uncertainties. The present results are not completely compatible with the previously published OPAL results [2]. The present results supersede the previously published results, because we now have a better understanding of the behaviour of the resonance decay products which affect the reference sample, and of the systematic uncertainties related to the track selection. The results show some differences compared to the values of $R_{\rm G}$ and $\lambda_{\rm G}$ obtained by other LEP experiments [4, 30]. Most of the differences seem to arise from different track selections, different purities and different choices of the reference sample.

Since the chaoticity parameter λ is expected to be dependent on the sample purity, the analysis was repeated with the $\mathrm{d}E/\mathrm{d}x$ measurements being used to vary the pion purity of the sample. An increase in $\lambda_{\rm G}$ with increasing pion purity was observed, while $R_{\rm G}$ was found to be unchanged.

3.2 Results using the Kopylov–Podgoretskiĭ parametrisation

The analysis was repeated using the KP parametrisation. As was mentioned earlier, the q_t distributions were obtained after restricting q_0, the absolute value of the energy difference of the two pions, to be less than $q_{0\,max} = 0.20\,{\rm GeV}$. This cut reduced the size of the data sample by approximately a factor of 10.

As in the G parametrisation fit, we excluded the region $q_t < 0.05$ GeV/c to avoid problems of detector resolution and split tracks, and the regions $0.275 < q_t < 0.45$ GeV/c,

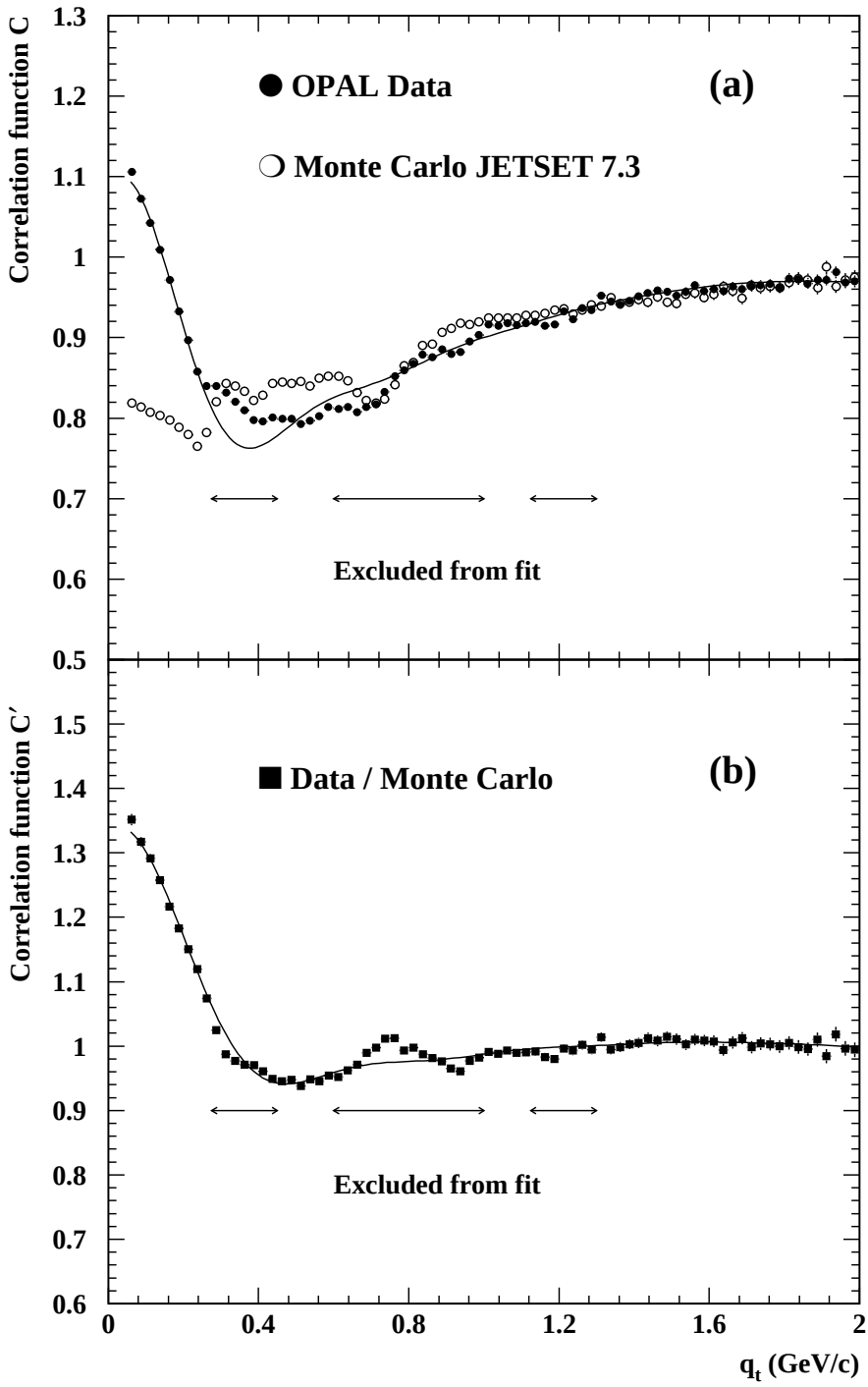

Figure 2: (a) The correlation function $C(q_t)$ for like charged pairs relative to unlike charged pairs. Solid points indicate the Coulomb corrected data, open points Monte Carlo events with full detector simulation. (b) The correlation function $C'(q_t)$ obtained by dividing the two distributions in (a). In (a) and (b) the solid lines show the fits to the KP parametrisation. The regions excluded from the reference fits are indicated in the figures. The error bars represent the statistical uncertainties.

	$R_{\rm KP}$ (fm)	$\lambda_{\rm KP}$	χ^2/d.o.f.
a) Reference fit	1.778 ± 0.023	0.719 ± 0.024	271/40
b) $q_0 < 0.15$ GeV	1.783 ± 0.023	0.746 ± 0.027	235/40
c) Different resonance regions excl.	1.752 ± 0.019	0.695 ± 0.020	319/49
d) Modified track selection	1.754 ± 0.026	0.722 ± 0.028	217/40
e) q_t binning = 50 MeV/c	1.778 ± 0.029	0.713 ± 0.031	183/22
f) $0.05 \leq q_t \leq 1.5$ GeV/c	1.783 ± 0.032	0.690 ± 0.049	248/20
g) Ref. sample from Monte Carlo	1.489 ± 0.018	0.637 ± 0.010	40.1/40

Table 2: Results of several fits of the KP parametrisation to the data, with statistical errors. These results were used to estimate the overall systematic uncertainties on the parameters. The differences between the parameter values of the reference fit (a) and the others from (b) to (f) were added in quadrature to obtain an estimate of the systematic errors on $R_{\rm KP}$ and $\lambda_{\rm KP}$. The errors have been scaled by $(\chi^2/\text{d.o.f.})^{1/2}$.

$0.6 < q_t < 1.0$ GeV/c, and $1.1 < q_t < 1.3$ GeV/c because of large distortions in the correlation function due to resonance decays (see Fig. 2a). The result of the fit[3] is given in line (a) of Table 2. Checks similar to the ones of the G parametrisation analysis were performed in order to estimate the systematic errors, and are summarised in Table 2.

In order to estimate the q_{0max} dependence, we varied the q_{0max} value from 0.20 GeV to 0.15 GeV, obtaining the $R_{\rm KP}$ and $\lambda_{\rm KP}$ values given in fit (b) of Table 2. A fit (c) was made excluding different resonance regions, as in Section 3.1. It can be seen that the shifts in fit parameters are small. The analysis was repeated changing the track selection criteria, as described in Section 2, in order to estimate systematic effects related to track and event selection (fit (d)). The resolution of the variable q_t is about 11 MeV/c, independent of the direction of the summed momentum of the tracks making up the pair. A study (fit (e)) of possible systematic effects due to the binning choice was performed by changing the bin size from 25 MeV/c to 50 MeV/c. In order to estimate the systematic uncertainties due to the long-range correlations of the distributions, a fit (f) was performed in a more restricted interval, $0.05 \leq q_t \leq 1.5$ GeV/c. The values of the parameters again show small shifts from the reference fit.

An estimate of the systematic uncertainties was obtained by summing in quadrature the differences of each fit (b)–(f) with the reference fit (a). The final results are

$$R_{\rm KP} = 1.778 \pm 0.023 \pm 0.036\,\text{fm}, \qquad \lambda_{\rm KP} = 0.719 \pm 0.024 \pm 0.047,$$

where the first errors are statistical and the second are estimates of systematic uncertainties. As expected, $R_{\rm KP}$ has a larger value than $R_{\rm G}$.

An alternative correlation function was obtained using the Monte Carlo data set, according to Eq. 7. Since the use of the Monte Carlo sample does not remove the problems related to the resonance decay products (see Fig. 2b), we do not use the results of this fit (line (g) in Table 2) to estimate the systematic error, as in the case of the Goldhaber parametrisation.

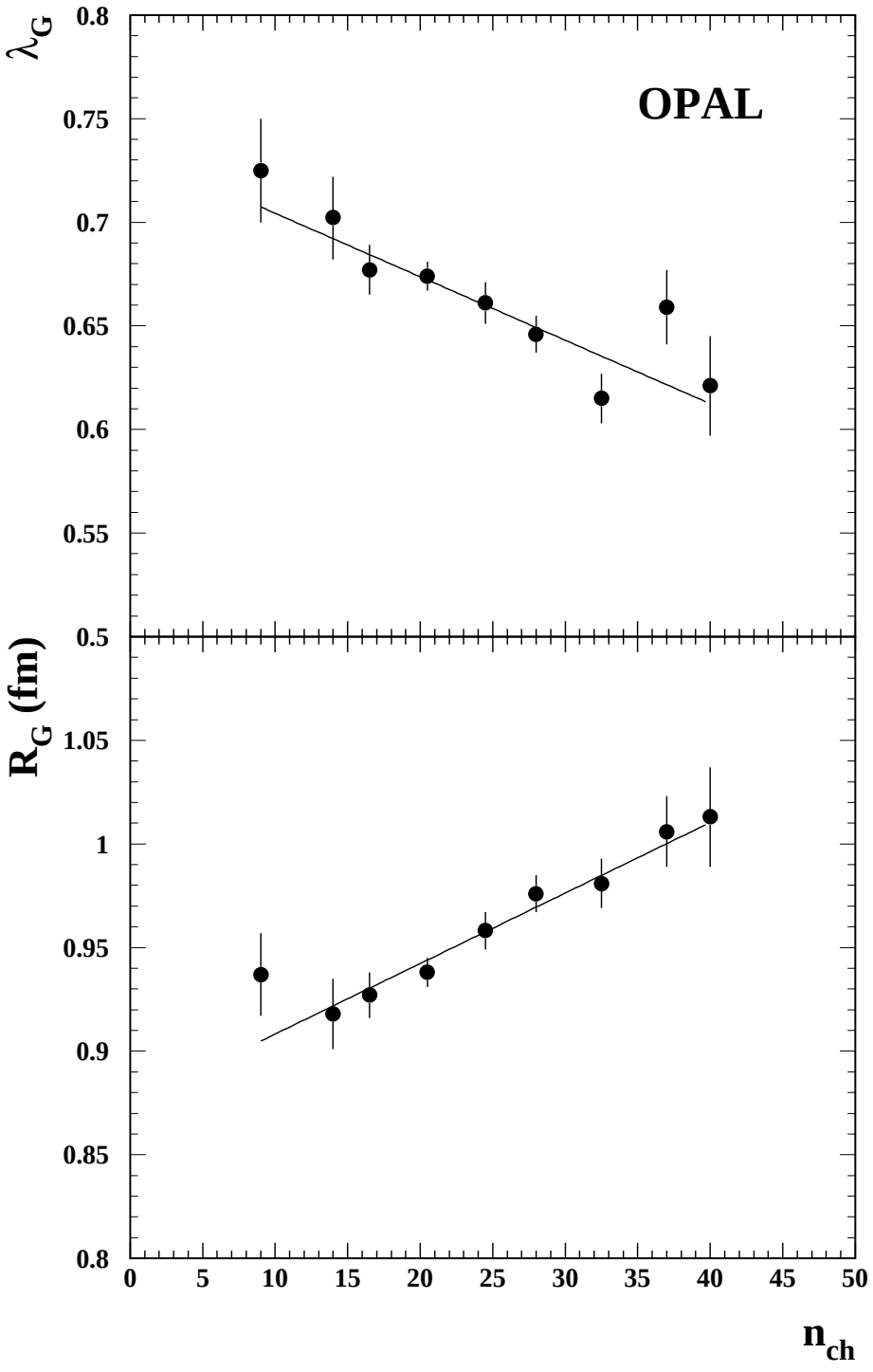

Figure 3: Dependence of the chaoticity parameter $\lambda_{\rm G}$ (upper plot) and the radius $R_{\rm G}$ (lower plot) on the average observed charged multiplicity, n_{ch}. The error bars represent statistical errors only. The lines represent fits described in the text.

4 Multiplicity dependence of R and of λ

4.1 Measurement of the multiplicity dependence

We have studied the dependence of the R and λ parameters on the observed charged multiplicity of the events, computed as described in Section 2. Events were grouped into nine multiplicity intervals. For each interval the analysis was repeated. As the like charged track sample and the reference sample were formed by pairing particles from the same event, the cut on multiplicity used to group events had the same effects on both samples. The results for the G parametrisation are summarised in Fig. 3, in which the errors shown are statistical only. The systematic errors due to the general cuts, described in Section 3, shift every point up or down by a similar amount and so do not affect the point to point behaviour.

Linear fits to the points of Fig. 3 were performed for $R_{\rm G}$ and $\lambda_{\rm G}$ as functions of n_{ch} ($R_{\rm G} = R'_{\rm G}\, n_{ch} + R^0_{\rm G}$, $\lambda_{\rm G} = \lambda'_{\rm G}\, n_{ch} + \lambda^0_{\rm G}$), in order to quantify the strength of this effect, and to compare our results obtained using the G and KP parametrisations. These fits yielded the following parameters:

$$\begin{array}{lll} R'_{\rm G} = (0.340 \pm 0.055) \cdot 10^{-2}\,{\rm fm}, & R^0_{\rm G} = 0.874 \pm 0.014\,{\rm fm}, & \chi^2/{\rm d.o.f.} = 4.2/7, \\ \lambda'_{\rm G} = -(0.306 \pm 0.058) \cdot 10^{-2}, & \lambda^0_{\rm G} = 0.735 \pm 0.015, & \chi^2/{\rm d.o.f.} = 8.7/7. \end{array}$$

As can be seen in Fig. 3, the radius $R_{\rm G}$ increases with multiplicity, while $\lambda_{\rm G}$ decreases. The fractional change of $R_{\rm G}$ with respect to a unit increase in n_{ch} is

$$\frac{1}{\langle R_{\rm G}\rangle}\frac{\Delta R_{\rm G}}{\Delta n_{ch}} = (3.6 \pm 0.6) \cdot 10^{-3}, \tag{8}$$

where $\langle R_{\rm G}\rangle$ is the radius value obtained from the inclusive event sample.

A similar analysis was also performed using the KP parametrisation. The results are summarised in Fig. 4. Linear fits have been performed to the values of $R_{\rm KP}$ and $\lambda_{\rm KP}$ as functions of n_{ch} ($R_{\rm KP} = R'_{\rm KP}\, n_{ch} + R^0_{\rm KP}$, $\lambda_{\rm KP} = \lambda'_{\rm KP}\, n_{ch} + \lambda^0_{\rm KP}$), and gave the following results:

$$\begin{array}{lll} R'_{\rm KP} = (0.61 \pm 0.17) \cdot 10^{-2}\,{\rm fm}, & R^0_{\rm KP} = 1.638 \pm 0.043\,{\rm fm}, & \chi^2/{\rm d.o.f.} = 4.1/7, \\ \lambda'_{\rm KP} = -(0.131 \pm 0.016) \cdot 10^{-2}, & \lambda^0_{\rm KP} = 1.037 \pm 0.047, & \chi^2/{\rm d.o.f.} = 5.5/7. \end{array}$$

The fractional increase per unit multiplicity of the radius $R_{\rm KP}$ is consistent with that of the radius $R_{\rm G}$

$$\frac{1}{\langle R_{\rm KP}\rangle}\frac{\Delta R_{\rm KP}}{\Delta n_{ch}} = (3.4 \pm 1.0) \cdot 10^{-3}, \tag{9}$$

where $\langle R_{\rm KP}\rangle$ is the radius value measured in the inclusive event sample. The values of $\lambda_{\rm KP}$ decrease more strongly with increasing n_{ch} than for $\lambda_{\rm G}$. These two observations are similar to what has been observed in hadron-hadron experiments [5, 6, 7] which used the KP parametrisation to describe the correlation function. It should be pointed out that a consistent increase of the radius with multiplicity is observed also when using the ratio of Eq. 7, that is when normalising to the Monte Carlo.

[3] The other parameter values of the fit are $\delta_{\rm KP} = 0.541 \pm 0.013\,({\rm GeV/c})^{-1}$, $\epsilon_{\rm KP} = -0.1423 \pm 0.0055\,({\rm GeV/c})^{-2}$, $N_{\rm KP} = 0.6409 \pm 0.0031$, where the errors given are those from the fit, not scaled by $(\chi^2/{\rm d.o.f.})^{1/2}$.

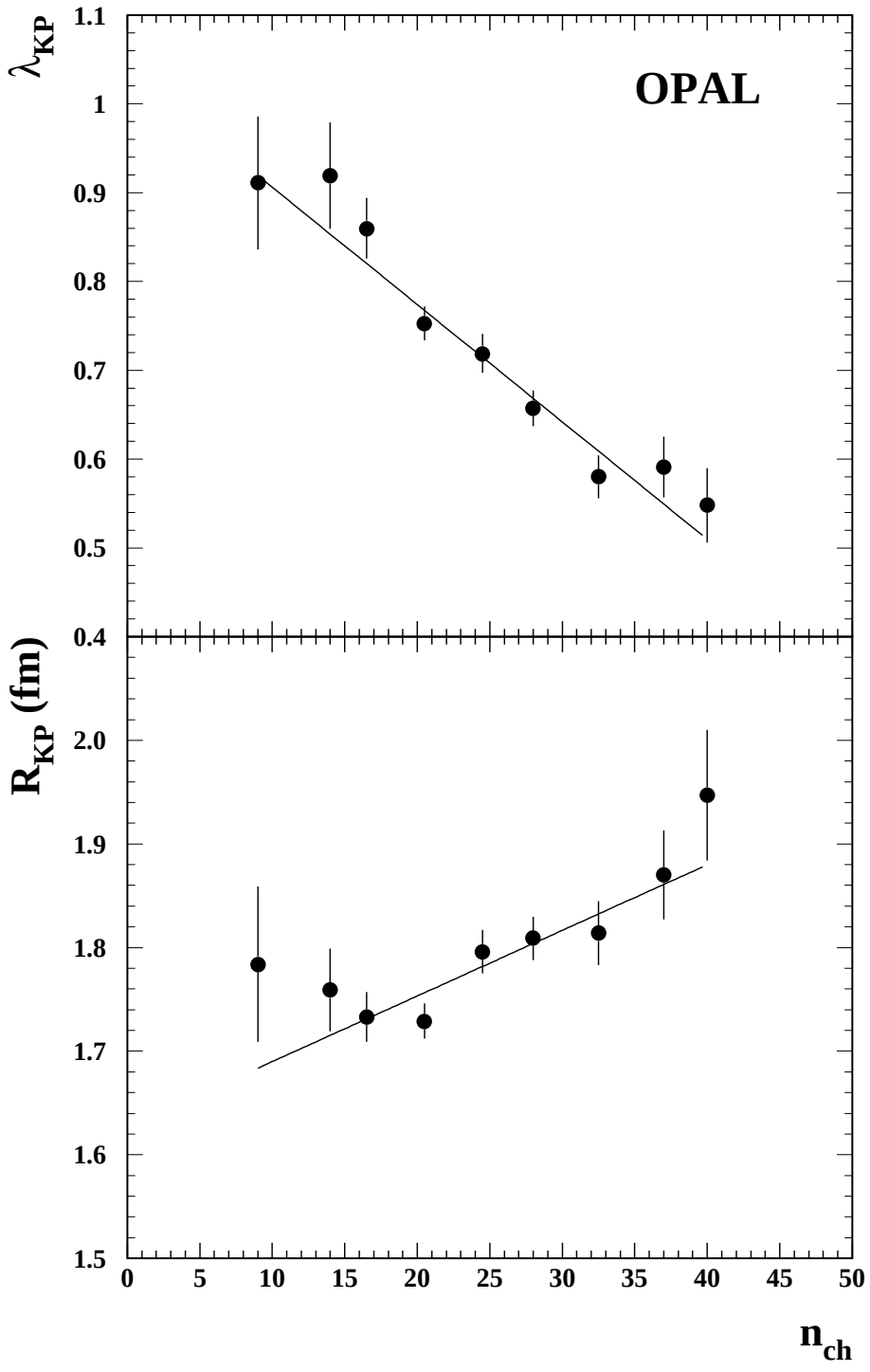

Figure 4: Dependence of the chaoticity parameter $\lambda_{\rm KP}$ (upper plot) and of the radius $R_{\rm KP}$ (lower plot) on the average observed charged multiplicity, n_{ch}. The error bars represent statistical errors only. The lines represent fits described in the text.

4.2 Discussion of the multiplicity dependence

In order to search for possible experimental biases which might induce the multiplicity dependence of the radius and chaoticity parameters, and to search for possible correlations with other event properties, we have performed several studies.

As we found a dependence of λ on the average momentum $\langle p \rangle$ of tracks, we first searched for a possible correlation of the radius and λ with $\langle p \rangle$ of the tracks in an event, since the average momentum decreases with increasing n_{ch}. We divided the $\langle p \rangle$ distribution into six intervals and determined $R_{\rm G}$ and $\lambda_{\rm G}$ in each momentum range. The value of $\lambda_{\rm G}$ was observed to decrease strongly with the average track momentum $\langle p \rangle$, while it decreased with charged multiplicity. The radius $R_{\rm G}$ did not show any strong dependence on $\langle p \rangle$, while it increased with charged multiplicity.

The purity of the the pion sample was found to increase slightly with the observed charged multiplicity. As we already mentioned in Section 3.1, the λ value increases with increasing pion purity, so that the decreasing value of λ cannot be explained by a different pion purity in the multiplicity bins.

Another possible explanation of the multiplicity effect could be found in the different values that R and λ have in samples with different numbers of reconstructed jets. We performed the BE analysis on three samples in which events were selected by the number of jets found with the JADE 'E0' algorithm [31] using charged tracks only, and in which two, three, and four jets were reconstructed. For each sample we determined $\lambda_{\rm G}$ and $R_{\rm G}$. For a better evaluation of the systematic effects related to the choice of the jet resolution parameter y_{cut}, the value of y_{cut} was set at four different values ranging from $y_{cut} = 0.01$ to $y_{cut} = 0.04$. The results are shown in Fig. 5. The size of the emitting region becomes larger as the number of jets increases, and the differences among the $R_{\rm G}$ values remain approximately the same for any value of y_{cut}. The chaoticity parameter $\lambda_{\rm G}$ shows a higher value in two-jet events compared to the values obtained in three- and four-jet events. The same analysis was repeated for the KP parametrisation, giving comparable results.

The multiplicity analysis was then performed on two samples in which events were selected by the number of jets found using $y_{cut} = 0.03$. The first sample contained two-jet events and the second sample three-jet events. As can be seen in Fig. 6, three-jet events have larger radius values for both the G and the KP parametrisations. Furthermore, the dependence of R on charged multiplicity seems to be less strong for the exclusive two-jet and three-jet selected samples than for the inclusive sample without any jet selection. This effect could partially explain the rise of the radius with charged multiplicity. At low values of n_{ch}, the composition of the event sample is dominated by two-jet events, which have lower radius values, while at high values of n_{ch} the three-jet events dominate. The overall effect is an increase of the radius with n_{ch} in the inclusive sample. As a cross-check, we repeated the analysis on the two- and three-jet event samples using $y_{cut} = 0.04$ and we found no significant differences in the results. The analysis was also performed using a cone jet finder [32]. The cone jet finder has an important feature with regard to the present work in that it does not use an invariant mass algorithm to determine the number of jets in an event. Again no significant differences were found from the results presented above.

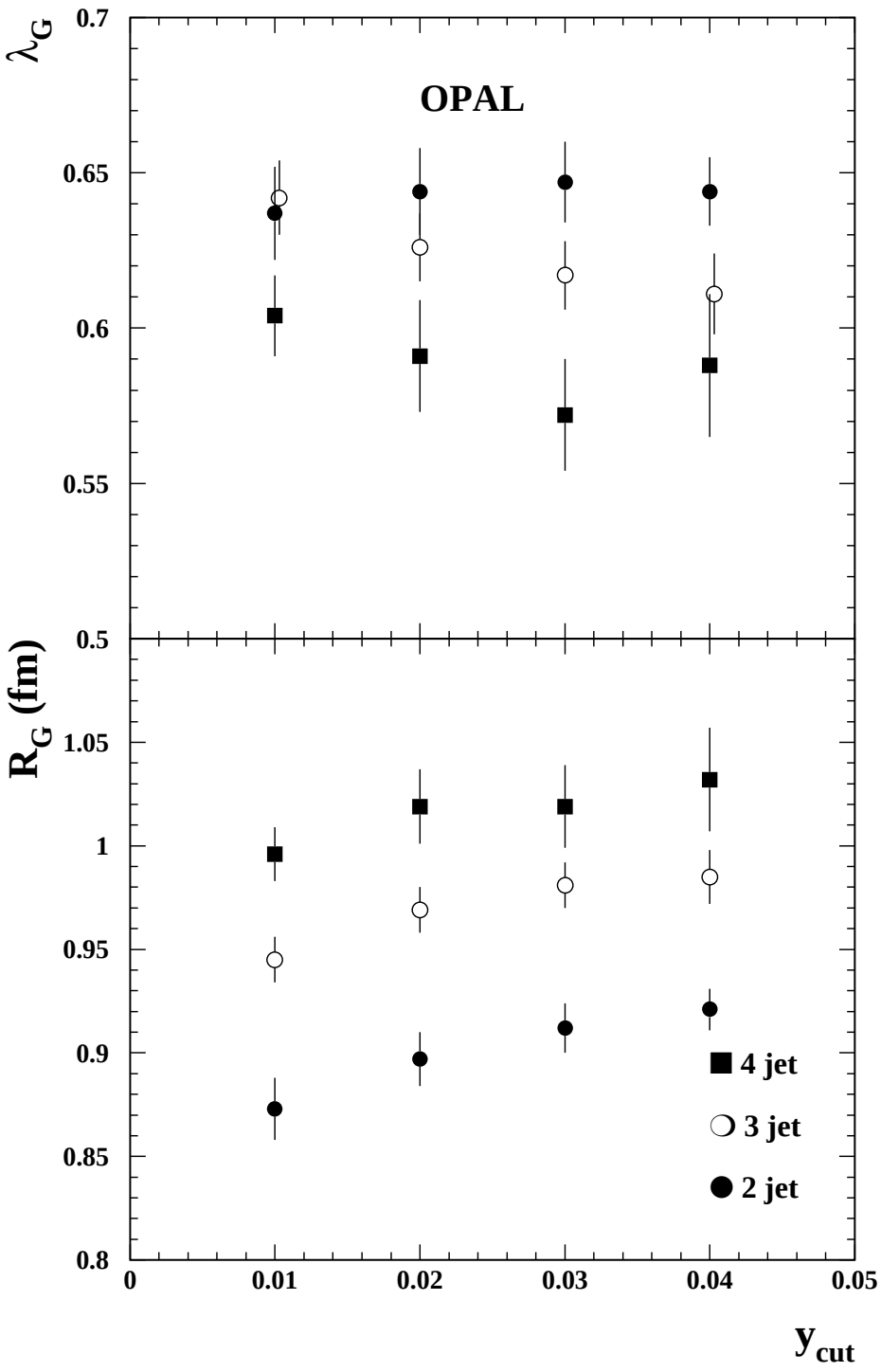

Figure 5: Dependence of $\lambda_{\rm G}$ (upper plot) and $R_{\rm G}$ (lower plot) on y_{cut} for two-jet (solid points), three-jet (open points), and four-jet events (solid squares) found using the JADE 'E0' algorithm. The values of $R_{\rm G}$ are higher in four- and in three-jet events than in two-jet events, while $\lambda_{\rm G}$ has lower values in three-jet events than in two-jet events. Lines represent linear fits to the R and λ values as functions of n_{ch}. The error bars represent the statistical errors only.

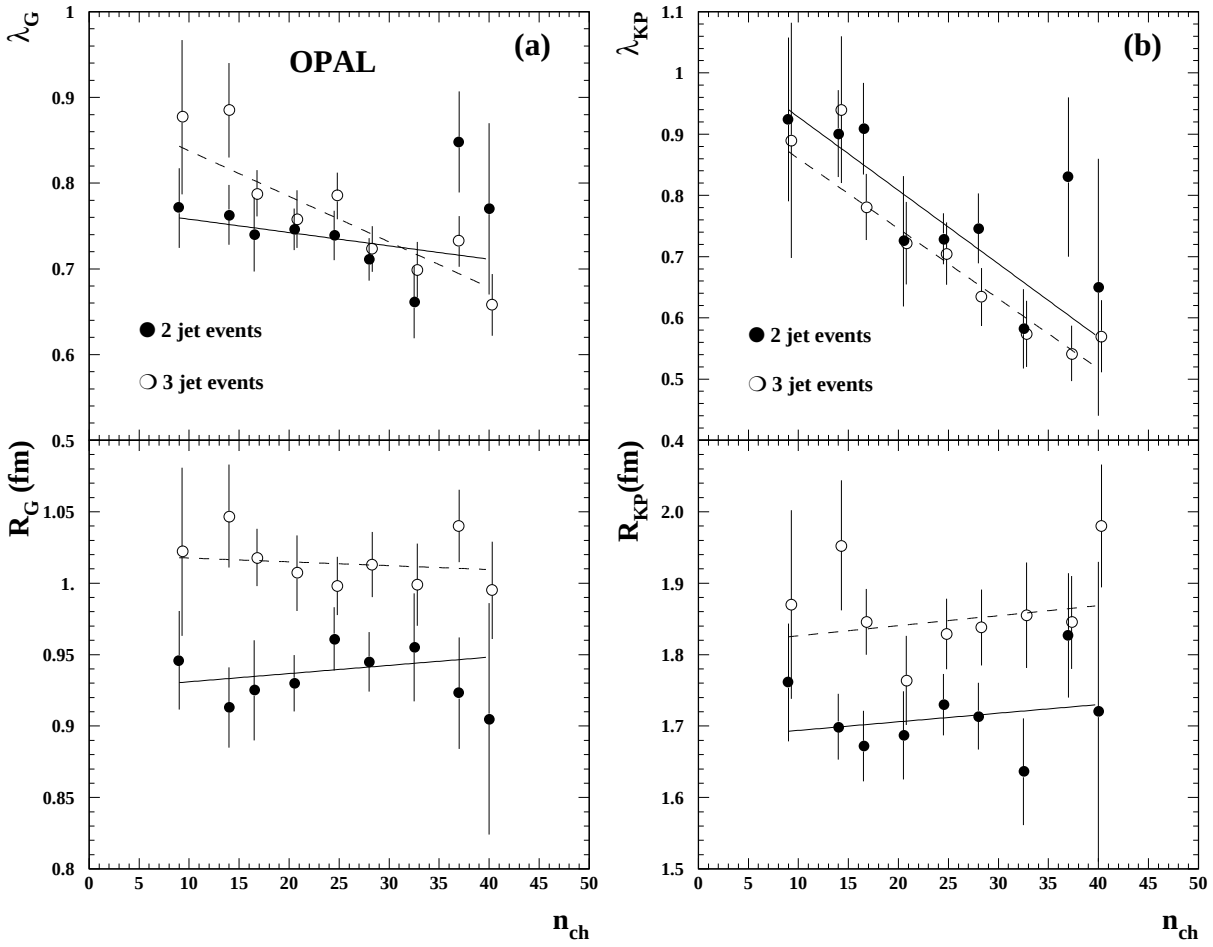

Figure 6: Dependence of R and λ on the average observed charged multiplicity, n_{ch}, for two-jet event (solid points) and three-jet events (open points). The results of the fits performed using the G parametrisation are plotted in (a) and those for the KP parametrisation in (b). The error bars represent the statistical errors only. The solid lines represent linear fits to the two-jet event points and the dashed lines represent linear fits to the three-jet event points.

5 Conclusions

We have measured the average radius of the emitting source R and the chaoticity parameter λ for both the Goldhaber (G) and the one-dimensional Kopylov-Podgoretskiĭ (KP) parametrisations of the Bose–Einstein correlations for the entire event sample of hadronic Z^0 decays, in which 79% of the tracks used are pions. We find:

$$R_{\rm G} = 0.955 \pm 0.012(\text{stat.}) \pm 0.015(\text{syst.})\,\text{fm}, \quad \lambda_{\rm G} = 0.672 \pm 0.013(\text{stat.}) \pm 0.024(\text{syst.}),$$

$$R_{\rm KP} = 1.778 \pm 0.023(\text{stat.}) \pm 0.036(\text{syst.})\text{fm}, \quad \lambda_{\rm KP} = 0.719 \pm 0.024(\text{stat.}) \pm 0.047(\text{syst.}).$$

The measured $R_{\rm G}$ and $R_{\rm KP}$ are different, as expected on the basis of the different assumptions about the shape of the pion radiating source.

We have studied the dependence of the radius and of the chaoticity parameter on the observed charged multiplicity for the two different parametrisations. The radii are found to increase with charged multiplicity, n_{ch}, as

$$\frac{1}{\langle R_{\rm G}\rangle}\frac{\Delta R_{\rm G}}{\Delta n_{ch}} = (3.6 \pm 0.6)\cdot 10^{-3} \quad \text{and} \quad \frac{1}{\langle R_{\rm KP}\rangle}\frac{\Delta R_{\rm KP}}{\Delta n_{ch}} = (3.4 \pm 1.0)\cdot 10^{-3},$$

where the $\langle R\rangle$ are the average radius values measured in the inclusive event sample. An increasing radius with increasing multiplicity has been measured in hadron-hadron experiments with centre-of-mass energies $\sqrt{s} \geq 30$ GeV [5, 6, 7]. This effect has also been observed in heavy ion collisions [8]. In separate samples of two-jet and three-jet events, the multiplicity dependence of the radius of the emitting source is reduced, the average value of R for three-jet events being larger than that for two-jet events by approximately 10%. The multiplicity difference of two- and three-jet events therefore could partly account for the increase of the radii $R_{\rm G}$ and $R_{\rm KP}$ with n_{ch}, since for low charged multiplicity the two-jet events make up most of the event sample, while for high n_{ch} the three-jet events dominate.

Acknowledgements

We particularly wish to thank the SL Division for the efficient operation of the LEP accelerator and for their continuing close cooperation with our experimental group.In addition to the support staff at our own institutions we are pleased to acknowledge the
Department of Energy, USA,
National Science Foundation, USA,
Particle Physics and Astronomy Research Council, UK,
Natural Sciences and Engineering Research Council, Canada,
Israel Ministry of Science,
Israel Science Foundation, administered by the Israel Academy of Science and Humanities,
Minerva Gesellschaft,
Japanese Ministry of Education, Science and Culture (the Monbusho) and a grant under the Monbusho International Science Research Program,
German Israeli Bi-national Science Foundation (GIF),
Direction des Sciences de la Matière du Commissariat à l'Energie Atomique, France,
Bundesministerium für Bildung, Wissenschaft, Forschung und Technologie, Germany,
National Research Council of Canada,
Hungarian Foundation for Scientific Research, OTKA T-016660, and OTKA F-015089.

References

[1] E. A. De Wolf, *On Bose–Einstein correlations and generating functions*, Proceedings of the XXIV Int. Symp. on Multiparticle Dynamics, Eds. A. Giovannini, S. Lupia and R. Ugoccioni, World Scientific, Singapore (1994) 15;
S. Haywood, *Where are we going with Bose–Einstein – a mini review*, RAL-94-074.

[2] OPAL Collab., P. D. Acton *et al.*, Phys. Lett. **B 267** (1991) 143.

[3] TPC Collab., H. Aihara *et al.*, Phys. Rev. **D 31** (1985) 996.

[4] ALEPH Collab., D. Decamp *et al.*, Z. Phys. **C 54** (1992) 75.

[5] AFS Collab., T. Åkesson *et al.*, Phys. Lett. **B 129** (1983) 269;
AFS Collab., T. Åkesson *et al.*, Phys. Lett. **B 187** (1987) 420.

[6] SFM Collab., A. Breakstone *et al.*, Z. Phys. **C 33** (1987) 333.

[7] UA1 Collab., C. Albajar *et al.*, Phys. Lett. **B 226** (1989) 410.

[8] NA35 Collab., A. Bamberger *et al.*, Z. Phys. **C 38** (1988) 79.

[9] G. D. Lafferty, Z. Phys. **C 60** (1993) 659.

[10] G. Goldhaber, S. Goldhaber, W. Lee, and A. Pais, Phys. Rev. Lett. **3** (1959) 181.

[11] G. I. Kopylov and M. I. Podgoretskiĭ, Sov. J. Nucl. Phys. **18** (1973) 656.

[12] G. Cocconi, Phys. Lett. **B 49** (1974) 459.

[13] EHS/NA22 Collab., N. M. Agababian *et al.*, Z. Phys. **C 59** (1993) 195.

[14] OPAL Collab., K. Ahmet *et al.*, Nucl. Instr. Methods **A 305** (1991) 275.

[15] P. P. Allport *et al.*, Nucl. Instr. Methods, **A324** (1993) 34;
P. P. Allport *et al.*, Nucl. Instr. Methods, **A346** (1994) 476.

[16] M. Hauschild *et al.*, Nucl. Instr. Methods **A 314** (1992) 174.

[17] OPAL Collab., M. Arignon *et al.*, Nucl. Instr. Methods **A 313** (1992) 103.

[18] OPAL Collab., G. Alexander *et al.*, Z. Phys. **C 52** (1991) 175.

[19] T. Sjöstrand, Comp. Phys. Comm. **39** (1986) 347;
T. Sjöstrand and M. Bengtsson, Comp. Phys. Comm. **43** (1987) 367.

[20] OPAL Collab., P. D. Acton *et al.*, Z. Phys. **C 58** (1993) 387;
OPAL Collab., M. Z. Akrawy *et al.*, Z. Phys. **C 47** (1990) 505.

[21] J. Allison *et al.*, Nucl. Instr. Methods **A 317** (1992) 47.

[22] OPAL Collab., R. Akers *et al.*, Phys. Lett. **B 320** (1994) 417.

[23] OPAL Collab., P. D. Acton *et al.*, Z. Phys. **C 60** (1993) 579.

[24] OPAL Collab., R. Akers *et al.*, Z. Phys. **C 65** (1995) 17.

[25] M. Gyulassy *et al.*, Phys. Rev. **C 20** (1979) 2267.

[26] M. G. Bowler, Phys. Lett. **B 270** (1991) 69.

[27] M. Biyajima, T. Mizoguchi, T. Osada, and G. Wilk, Phys. Lett. **B 353** (1995) 340.

[28] L. Montanet *et al.*, Phys. Rev. **D 50** (1994) 1173.

[29] OPAL Collab., P. Acton *et al.*, Z. Phys. **C 56** (1992) 521.

[30] DELPHI Collab., P. Abreu *et al.*, Phys. Lett. **B 286** (1992) 201;
DELPHI Collab., P. Abreu *et al.*, Z. Phys. **C 63** (1994) 17.

[31] JADE Collab., W. Bartel *et al.*, Z. Phys. **C 33** (1986) 23;
JADE Collab., S. Bethke *et al.*, Phys. Lett. **B 213** (1988) 235.

[32] OPAL Collaboration, R. Akers *et al.*, Z. Phys. **C63** (1994) 197.